JOURNAL OF PROPULSION AND POWER
Vol. 16, No. 3, May–June 2000

Flame/Stretch Interactions of Premixed Fuel-Vapor/O_2/N_2 Flames

O. C. Kwon,* M. I. Hassan,† and G. M. Faeth‡
University of Michigan, Ann Arbor, Michigan 48109-2140

Unstretched laminar burning velocities and flame response to stretch (Markstein numbers) were measured for outwardly propagating spherical laminar premixed flames involving mixtures of hydrocarbon vapors, oxygen, and nitrogen. Experimental conditions consisted of vapors of several liquid fuels (n-hexane, n-heptane, iso-octane, methyl-alcohol, and ethyl-alcohol), concentrations of oxygen in the nonfuel gases of 19–33% by volume, pressures of 0.5–2.0 atm, fuel-equivalence ratios of 0.80–1.60, and reactant mixture temperatures of 298 ± 5 K. The present flames were very sensitive to flame stretch, yielding ratios of unstretched to stretched laminar burning velocities in the range 0.4–4.0 for levels of flame stretch well below quenching conditions (Karlovitz numbers less than 0.2). At low pressures, the present hydrocarbon vapor flames had positive Markstein numbers at fuel-lean conditions, which is consistent with classical preferential-diffusion ideas. Increasing pressures, however, reduced Markstein numbers and progressively decreased the fuel-equivalence ratio range where Markstein numbers were positive. Negative Markstein numbers were associated with the presence of preferential-diffusion instability as evidenced by the appearance of chaotically distorted (wrinkled) flame surfaces early during the flame propagation process.

Nomenclature

D	= mass diffusivity
K	= flame stretch or normalized increase of flame surface area, Eq. (3)
Ka	= Karlovitz number, $K D_u / S_L^2$
L	= Markstein length
Ma	= Markstein number, L / δ_D
P	= pressure
r_f	= flame radius
S_L	= laminar burning velocity based on unburned gas properties
S'_L	= value of S_L at the largest radius observed
T	= temperature
t	= time
δ_D	= characteristic flame thickness, D_u / S_L
ρ	= density
ϕ	= fuel-equivalence ratio

Subscripts

b	= burned gas
max	= maximum observed value
u	= unburned gas
∞	= unstretched flame condition

Introduction

RECENT studies show that preferential diffusion of mass and heat cause laminar premixed flames to be sensitive to flame stretch.[1–10] Most of these studies considered gaseous fuels, for example, hydrogen, wet carbon monoxide, methane, ethane, ethylene, propane, etc., which raises questions about the behavior of premixed flames fueled with the vapors of liquid fuels that are important for aerospace and ground transportation systems, among others. Thus, the present objective was to study premixed-flame/stretch interactions of flames fueled with the vapors of liquid fuels (n-hexane, n-heptane, iso-octane, methyl alcohol, and ethyl alcohol) in oxygen and nitrogen mixtures. Outwardly propagating spherical laminar premixed flames were observed to find the laminar burning velocities of unstretched flames and the sensitivity of laminar burning velocities to flame stretch as characterized by Markstein numbers. Experimental conditions included oxygen/nitrogen mixtures with concentrations of oxygen of 19–33% by volume, pressures of 0.5–2.0 atm, fuel-equivalence ratios of 0.80–1.60, and reactant mixture temperatures of 298 ± 5 K. The following description of the study is brief, see Refs. 4–9 and references cited therein for more details.

The present experiments were analyzed to find preferential-diffusion/stretch interactions similar to the studies of outwardly propagating spherical laminar premixed flames described in Refs. 4–9. As before, problems of flame thickness variations, curvature, and unsteadiness caused by variations of laminar burning velocities with increasing flame radius were minimized by only considering conditions where $\delta_D / r_f \ll 1$ and effects of ignition disturbances and radiative heat losses are small.[5,7] Then, the relationship between the laminar burning velocity and flame stretch can be represented conveniently as follows[4,11]:

$$S_{L_\infty} / S_L = 1 + MaKa \tag{1}$$

where the dimensionless Karlovitz number Ka and Markstein number Ma characterize flame stretch and the response of the flame to stretch, respectively. The values of S_L and Karlovitz number Ka were found following Strehlow and Savage,[12] based on predicted burned gas properties found using the computer codes of McBride et al.[13] and Reynolds.[14]

Several other proposals have been made to represent effects of flame stretch on laminar burning velocities (see Refs. 1, 2, and 10 and references cited therein); nevertheless, Eq. (1) is convenient because Markstein number has proven to be relatively constant for wide ranges of Karlovitz number so that S_{L_∞} and Markstein number provide concise measures of premixed flame propagation rates and response to stretch. The small stretch limit of Eq. (1) is also of interest, in order to connect present results to classical asymptotic theories of laminar premixed flame propagation; this expression can be found from Eq. (1) as follows[7]:

$$S_L / S_{L_\infty} = 1 - Ma_\infty Ka_\infty, \qquad Ka_\infty \ll 1 \tag{2}$$

where $Ma_\infty \approx Ma$, as noted earlier. Other advantages of the present characterization of premixed-flame/stretch interactions can be summarized as follows.[7] Data reduction is direct and does not involve the use of flame structure models that are difficult to fully define

Received 11 January 1999; revision received 12 May 1999; accepted for publication 2 June 1999.

*Graduate Student Research Assistant, Department of Aerospace Engineering.

†Visiting Scholar, Department of Aerospace Engineering; currently Lecturer, Mechanical Power Department, Helwan University, P.O. Box 11718, Mattaria, Cairo, Egypt.

‡Professor, Department of Aerospace Engineering; gmfaeth@umich.edu. Fellow AIAA.

Table 1 Summary of earlier laminar burning velocity measurements for premixed liquid-fuel-vapor/O/N flames

Source	Method	Pressure, atm	Equivalence ratio	O_2 concentration, % vol.[b]	Temperature, K
		n-Hexane/air			
Gerstein et al.[16]	Horizontal tube	1.0	1.01–1.29	21	298
Golovina and Fyodorov[21]	Bunsen burner	1.0	0.17–2.85	16–100	298
		n-Heptane/air			
Gerstein et al.[16]	Horizontal tube	1.0	0.99–1.34	21	298
Heimel and Weast[20]	Bunsen burner	1.0	0.86–1.28	21	308–579
Gibbs and Calcote[22]	Bunsen burner	1.0	0.70–1.40	21	298, 373
Davis and Law[29]	Twin flame[a]	1.0	0.70–1.70	21	298
		Iso-Octane/air			
Von Sachsse and Bartholome[15]	Bunsen burner	1.0	1.07	21	293
Dugger and Graab[17]	Bunsen burner	1.0	1.00–1.05	21–50	311, 422
Van Franze and Wagner[19]	Bunsen burner	1.0	1.09	21	293
Heimel and Weast[20]	Bunsen burner	1.0	0.85–1.18	21	298–707
Gibbs and Calcote[22]	Bunsen burner	1.0	0.80–1.30	21	298, 373
Gülder[23]	Spherical chamber	1.0–7.9	0.75–1.35	21	300–500
Metghalchi and Keck[24]	Spherical chamber	0.4–50	0.80–1.50	16–21	298–700
Bradley et al.[10]	Spherical chamber[a]	1.0–9.9	0.80–1.30	21	358–450
Davis and Law[29]	Twin flame[a]	1.0	0.07–1.70	21	298
		Methyl-alcohol/air			
Wiser and Hill[18]	Horizontal tube	0.9	0.17–1.79	21–100	300
Van Franze and Wagner[19]	Bunsen burner	1.0	1.09	21	293
Gibbs and Calcote[22]	Bunsen burner	1.0	0.70–1.40	21	298, 373
Gülder[23]	Spherical chamber	1.0–7.9	0.70–1.40	21	300–500
Metghalchi and Keck[24]	Spherical chamber	0.4–50	0.80–1.20	21	298–700
Egolfopoulos et al.[27]	Twin flame[a]	1.0	0.50–1.97	21	298–368[c]
		Ethyl-alcohol/air			
Gülder[23]	Spherical chamber	1.0–7.9	0.70–1.40	21	300–500
Egolfopoulos et al.[28]	Twin flame[a]	1.0	0.55–1.82	21	298–453[c]

[a]Stretch-corrected laminar burning velocities; Bradley et al.[10] also report Markstein numbers.
[b]Concentration of oxygen in the nonfuel gases.
[c]Extrapolated to reach 298 K.

and are likely to be revised in the future; the characterization is concise, which facilitates its use by others; the positive and negative ranges of Markstein numbers provide a direct indication of stable and unstable flame surface conditions with respect to effects of preferential diffusion; and the results can be readily transformed to provide direct comparisons with other ways to characterize premixed-flame/stretch interactions. Note, however, that the present approach has only been applied to outwardly propagating spherical laminar premixed flames when δ_D / r_f, effects of ignition disturbances and effects of radiation are all small. Thus, direct use of the present Markstein number to characterize effects of flame stretch for other circumstances should be approached with caution.

The properties of the laminar burning velocities of premixed fuel-vapor/air mixtures for the present liquid fuels have been considered earlier (see Refs. 10, 15–29 and references cited therein and the summary of Table 1). Bradley et al.[10] studied outwardly propagating laminar premixed flames, finding unstretched laminar burning velocities and Markstein numbers for mixtures of air and vapors of iso-octane and iso-octane/n-heptane blends. Their methods of data reduction differed from methods used here and in earlier related studies,[4–9] but their results do suggest strong response to stretch for reactant mixtures fueled with hydrocarbon vapors. Independent confirmation of these results is needed, however, due to the importance of these findings. Egolfopoulos et al.[27,28] and Davis and Law[29] also considered effects of stretch on laminar burning velocities, measuring laminar burning velocities for iso-octane, methyl-alcohol, and ethyl-alcohol vapors using the counterflow twin flame technique. Measurements at finite stretch rates were extrapolated using an empirical technique to find the fundamental laminar burning velocities of unstretched flames. Flame response to stretch, however, was not quantified during these studies. The other experimental studies summarized in Table 1 use a variety of techniques but do not consider effects of stretch. Thus, the laminar burning velocities that are reported involve considerable uncertainties about effects of stretch, particularly in view of the findings of Bradley et al.[10]

Because of the importance of premixed flames involving hydrocarbon-vapor/air mixtures, numerical simulations of such flames have received considerable attention. Studies along these lines, limited to detailed reaction mechanisms for experimental conditions considered during the present investigation, include Bradley et al.,[26] Egolfopoulos et al.,[27,28] Davis and Law,[29] Warnatz,[30] Lindstedt and Maurice,[31] Nehse et al.,[32] Pitsch et al.,[33] Held et al.,[34] and Müller et al.[35] The main features of these simulations are summarized in Table 2. Calculations using these detailed mechanisms are limited to the laminar burning velocities of unstretched flames. Egolfopoulos et al.,[27,28] Davis and Law,[29] and Müller et al.[35] use corresponding stretch-corrected unstretched laminar burning velocities to evaluate their predictions. The remaining studies, however, compare predictions with measurements of laminar burning velocities having unknown effects of stretch, which somewhat compromises the evaluation. Numerical simulations of premixed-flame/stretch interactions using detailed mechanisms require lengthy computation times, and none have yet been reported for the conditions considered during the present investigation. Müller et al.,[35] however, obtained predictions of premixed-flame/stretch interactions for iso-octane-fueled flames using a simplified approach that suggests rather strong sensitivity to stretch, in agreement with Bradley et al.[10]

Review of past work suggests that new measurements of unstretched laminar burning velocities and premixed-flame/stretch interactions are needed for reactant mixtures fueled with vapors of liquid fuels. Thus, the present investigation had the following objectives: 1) measure the properties of outwardly propagating spherical laminar premixed flames of fuel-vapor/O_2/N_2 mixtures at various pressures and standard temperature (298 K), 2) reduce the measurements to find characteristic laminar premixed flame properties (S_{L_∞} and Markstein number Ma), 3) compare the new measurements with existing measurements and numerical simulations, and 4) exploit the new measurements to gain insight about premixed-flame/stretch interactions.

Table 2 Summary of earlier laminar burning velocity predictions for premixed liquid fuel-vapor/air flames[a]

Source	Fuel vapors considered	Temperature, K	Mechanism	
			Number of species	Number of reactions
Bradley et al.[26]	Methyl-alcohol	300	17	40
Egolfopoulos et al.[27]	Methyl-alcohol	298	30	171
Egolfopoulos et al.[28]	Ethyl-alcohol	298	35	196
Davis and Law[29]	n-Heptane, Iso-octane	298	69	406
Warnatz[30]	n-Hexane, n-Heptane	298	31	97
Lindstedt and Maurice[31]	n-Heptane	298	109	659
Nehse et al.[32]	n-Heptane	298	>66	>197
Pitsch et al.[33]	Iso-octane	328	109	967
Held et al.[34]	n-Heptane	298	41	266
Müller et al.[35]	Methyl-alcohol,	298	33	116
	n-Heptane,	298	51	249
	Iso-octane	298	61	257

[a]Flame conditions are for 1 atm and are summarized for results plotted here; see original sources for complete range of flame conditions considered. These predictions were for unstretched flames having negligible heat losses although Müller et al.[35] find premixed-flame/stretch interactions using a simplified approach.

Experimental Methods

The present experiments were carried out in the spherical windowed chamber used for recent studies of laminar premixed-flame/stretch interactions.[4–9] The combustible mixture was prepared in the chamber and then spark ignited at the center of the chamber using minimum spark ignition energies to control ignition disturbances. The flames were observed using high-speed (up to 4000 pictures/s) motion picture shadowgraphy. Once combustion was completed, the chamber was vented and then flushed with air until it cooled to the allowable initial temperature range of the experiments [298 ± (3–5) K].

The test chamber was evacuated to begin preparing a mixture for a test. The appropriate volume of liquid fuel was then injected into the chamber using a gas-tight syringe. After fuel injection, the chamber was allowed to stand for 5–10 min to ensure complete evaporation of the fuel. The chamber was then filled with the desired O_2/N_2 mixture to the test pressure and mixed for 10 min using a small metal fan located within the chamber. After the fan was stopped, the motion of the gas within the chamber was allowed to decay for another 10 min before the mixture was ignited. Using these procedures, flame propagation was spherically symmetric with no evidence of significant flow disturbances in the unburned gas.

The present measurements were limited to flames having diameters greater than 10 mm to avoid ignition disturbances. Measurements were also limited to flames having diameters less than 60 mm so that pressure increases within the gas mixture were less than 0.4% of the initial gas pressure during the period when flame propagation rates were measured. No test results are reported in the following where the flame surface was distorted or wrinkled due to effects of buoyancy or flame instability. Measurements were limited to $\delta_D / r_f \leq 2\%$, similar to Refs. 4–9, so that effects of curvature and transient phenomena associated with large flame thicknesses were small. Finally, estimates showed that radiative heat losses were less than 5% of the rate of chemical energy release within the flames, implying small effects of radiation on flame properties. For these conditions, the laminar burning velocity and flame stretch are given by the following expressions[12]:

$$S_L = \frac{\rho_b}{\rho_u}\frac{\mathrm{d}r_f}{\mathrm{d}t}, \qquad K = \frac{2}{r_f}\frac{\mathrm{d}r_f}{\mathrm{d}t} \tag{3}$$

The density ratio needed in Eq. (3) was computed assuming adiabatic constant-pressure combustion with the same fuel-equivalence ratio (or concentrations of elements) in the unburned and burned gases. The computations to find the density ratios were completed using the algorithms of McBride et al.[13] and Reynolds,[14] with both yielding the same results. This approach agrees with past determinations of the properties of stretched laminar flames (see Refs. 4–9 and references cited therein); however, the use of the unstretched density ratio in this way is a convention that ignores preferential diffusion effects that modify local mixture fractions and thermal energy transport and cause local changes of the density ratios of stretched flames. The convention is convenient, however, because a single density ratio relates all flame speeds and laminar burning velocities; the present methods are unchanged from earlier work, which facilitates comparisons of measurements; and the approach retrieves the correct flame displacement velocity, $\mathrm{d}r_f/\mathrm{d}t$, for a particular flame condition and Karlovitz number. Given reliable structure predictions for various levels of stretch, however, density ratios should be computed as a function of stretch so that the actual laminar burning velocities and mass burning rates of these flames can be estimated.

Final results were obtained by averaging the measurements of 4–6 tests at each condition. Experimental uncertainties were estimated as described in Ref. 4 and references cited therein; the present uncertainties (95% confidence) are as follows: S_L less than 10%, Karlovitz number less than 20%, and Markstein number $|Ma|$ less than 25% for $|Ma| > 1$ and less than $25/|Ma|$% for $|Ma| < 1$. Present test conditions and major results are summarized in Table 3 for combustion in air at atmospheric pressure, in Table 4 for combustion in various oxygen/nitrogen mixtures at atmospheric pressure, and in Table 5 for combustion in air at various pressures.

Results and Discussion

Flame Stability and Evolution

Three kinds of flame surface instabilities were observed during the present investigation: preferential diffusion instability, hydrodynamic instability, and buoyant instability. Preferential diffusion instability (stability) was associated with negative (positive) Markstein numbers because bulges of the flame surface that are concave (convex) toward the combustion products have positive (negative) Karlovitz numbers [similar to Eq. (3) for spherical flames] and thus increased (decreased) laminar burning velocities through Eq. (1); as a result, the bulges grow (decay) and the flame is unstable (stable) to preferential diffusion effects. Hydrodynamic and buoyant instabilities were also observed; they are associated with effects of accelerating a light combustion product gas toward a heavy reactant gas as the flame propagates and effects of gravity introducing buoyant motion of the light combustion product gas in its heavy gas surroundings, respectively.

Shadowgraph photographs of flame surfaces after distortion by the three types of instabilities for outwardly propagating spherical flames appear in work by Kwon et al.[4] and Aung et al.[7] and references cited therein. The presence of preferential diffusion instability

Table 3 Test conditions for combustion in air at atmospheric pressure[a]

ϕ	ρ_u/ρ_b	$S'_{L\infty}$, mm/s	$S_{L\infty}$, mm/s	$\delta_{D\infty}$, μm	$K_{\max}$, s^{-1}	$Ka_{\max}$	Ma
n-Hexane/air: 298 ± 3 K, D_u = 7.78 mm²/s							
0.80	7.21	231	280	30	225	0.084	13.4
0.90	7.75	245	294	30	302	0.078	10.5
0.95	7.97	294	327	20	488	0.074	6.3
1.00	8.14	321	353	20	496	0.058	5.9
1.10	8.29	368	387	20	689	0.058	4.6
1.20	8.22	367	367	20	736	0.044	0.0
1.40	7.99	359	312	30	1009	0.037	−8.7
1.60	7.74	268	167	50	649	0.034	−16.8
n-Heptane/air: 298 ± 3 K, D_u = 6.92 mm²/s							
0.90	7.77	244	297	20	283	0.102	15.1
1.00	8.16	275	315	20	394	0.067	10.2
1.10	8.30	335	364	20	505	0.051	7.2
1.20	8.24	378	382	20	813	0.044	1.1
1.40	8.02	370	333	20	956	0.033	−7.5
1.60	7.77	307	230	30	705	0.029	−15.1
Iso-octane/air: 298 ± 3 K, D_u = 6.60 mm²/s							
0.90	7.76	203	247	30	166	0.153	16.8
1.00	8.16	262	312	20	344	0.083	12.8
1.10	8.30	288	325	20	446	0.061	8.3
1.20	8.23	317	336	20	476	0.037	3.9
1.40	8.00	307	290	20	613	0.035	−5.5
1.60	7.74	288	195	30	514	0.028	−16.5
Methyl-alcohol/air: 298 ± 3 K, D_u = 15.38 mm²/s							
0.80	7.17	244	244	60	567	0.149	0.0
0.90	7.65	305	305	50	831	0.132	0.0
1.00	8.00	353	353	40	987	0.124	0.0
1.10	8.11	410	402	40	1209	0.098	−0.5
1.20	8.04	440	401	40	1334	0.072	−3.4
1.40	7.85	433	361	40	1298	0.068	−4.9
Ethyl-alcohol/air: 298 ± 5 K, D_u = 11.95 mm²/s							
0.80	7.19	249	249	50	675	0.131	0.5
0.90	7.71	300	300	40	817	0.107	0.2
1.00	8.09	331	331	40	930	0.100	0.0
1.10	8.21	396	382	30	1247	0.084	−1.0
1.20	8.14	399	376	30	1371	0.074	−2.8
1.40	7.92	390	343	30	1426	0.065	−5.0

[a]Reactants at 1.0 atm.

Table 4 Summary of test conditions for n-hexane/O_2/N_2 flames[a]

$O_2/(O_2+N_2)$, %	ρ_u/ρ_b	$S'_{L\infty}$, mm/s	$S_{L\infty}$, mm/s	$\delta_{D\infty}$, μm	$K_{\max}$, s^{-1}	$Ka_{\max}$,	Ma
ϕ = 0.8							
21	7.21	231	280	30	225	0.084	13.4
23	7.63	284	323	20	392	0.067	8.5
25	8.02	392	422	20	599	0.043	6.1
27	8.37	482	501	20	862	0.037	4.8
29	8.68	573	583	10	1120	0.027	2.5
31	8.97	611	611	10	1230	0.026	0.0
33	9.23	706	706	10	1468	0.023	0.0
ϕ = 1.0							
19	7.71	240	268	30	337	0.072	6.2
21	8.14	321	353	20	496	0.058	5.9
23	8.53	412	434	20	757	0.043	4.5
25	8.89	504	504	20	992	0.030	0.0
27	9.21	583	582	10	1152	0.025	−0.1
29	9.51	679	680	10	1329	0.023	0.2
31	9.80	764	764	10	1585	0.021	0.0

[a]Reactants at 298 ± 4 K and 1.0 atm, D_u = 7.78 mm²/s.

could be identified by the development of irregular (chaotic) distortions of the flame surface relatively early in the flame propagation process. In contrast, hydrodynamic instability could be identified by the development of a somewhat regular cellular disturbance pattern on the flame surface rather late in the flame propagation process, similar to the observations of Groff[36] for propane/air flames. Finally, the appearance of buoyant instability was readily detected by distortion of the flame as a whole from a spherical shape as well as a tendency for the centroid of the flame image to move upward. Measurements were ended when flame surface distortions due these instabilities were observed. Typical of past work,[4–9] however, the onset of preferential diffusion instability was sufficiently delayed so that laminar burning velocities could be measured for a time in any event. Similarly, the onset of hydrodynamic and buoyant instabilities generally were observed at radii larger than the range of the measurements for present test conditions.

Table 5 Summary of test conditions for n-hexane/air flames at various pressures[a]

P, atm	ρ_u/ρ_b	$S'_{L\infty}$, mm/s	$S_{L\infty}$, mm/s	$\delta_{D\infty}$, μm	$K_{\max}$, s^{-1}	$Ka_{\max}$,	Ma
ϕ = 1.0							
0.5	8.08	374	440	40	399	0.098	7.1
1.0	8.14	321	353	20	496	0.058	5.9
1.5	8.17	304	312	20	568	0.036	2.0
2.0	8.20	291	291	10	547	0.026	−0.2

[a]Reactants at 298 ± 3 K, $D_u = 7.78/P$ (atm) mm²/s.

Fuel-Vapor/Air Flames at STP

Burning Velocity/Stretch Interactions

Similar to past observations,[4–9] values of S_L yielded linear plots when plotted as a function of Karlovitz number according to Eq. (1). This implies that the Markstein numbers were independent of Karlovitz number over the present test range and provided a straightforward interpolation to $Ka = 0$ to find $S_{L\infty}$. Then given $S_{L\infty}$, plots of $S_{L\infty}/S_L$ as a function of Karlovitz number were constructed as suggested by Eq. (1). On these plots, open symbols are used to denote neutral and stable preferential-diffusion conditions ($Ma \geq 0$) whereas filled symbols are used to denote unstable preferential-diffusion conditions ($Ma < 0$). The ranges of the measurements for strongly unstable conditions (large negative slopes or large negative Markstein numbers) are more abbreviated than the rest due to the relatively early transition to chaotically wrinkled flame surfaces. Present results involve rather modest values of flame stretch ($Ka < 0.2$), however, and are not close to extinction conditions where Karlovitz number would be on the order of unity and flame response to stretch is likely to change. Even for the present modest ranges of Karlovitz numbers, however, preferential diffusion/stretch interactions are substantial with values of $S_L/S_{L\infty}$ varying in the range 0.4–4.0. This implies strong flame-surface/turbulence interactions within turbulent premixed flames of these reactants, with turbulent distortion of flame surfaces being enhanced and retarded for unstable and stable preferential diffusion conditions, respectively.[4]

The results shown in Figs. 1–5 indicate that flame response to stretch is significantly greater for the paraffin vapors than for the alcohol vapors, whereas all of the vapors tend to be stable (unstable) for fuel-lean (-rich) conditions, respectively. These trends are in qualitative agreement with classical ideas about preferential diffusion/stretch interactions and stability in laminar premixed flames.[37,38] In particular, fuel mass diffusivities progressively decrease with increasing molecular weight tending to increase the potential for preferential diffusion effects for the paraffins compared to the much lighter alcohols (which have diffusivities similar to nitrogen and the other gases in these flames). Furthermore, fuel mass diffusivities, particularly for the heavier hydrocarbons, are smaller than the rest of the species in the flame, which implies a tendency for the mixture to become leaner with increasing stretch; this tends to decrease (increase) laminar burning velocities for fuel-lean (-rich) conditions, correspondingly leading to stable (unstable) preferential diffusion behavior. Other effects of flame temperatures and pressures on preferential diffusion/stretch interactions, however, appear to involve more complex behavior, as discussed later.

Unstretched Laminar Burning Velocities

Values of measured and predicted laminar burning velocities are plotted in Figs. 6–10. In Figs. 6–10, measured values of laminar

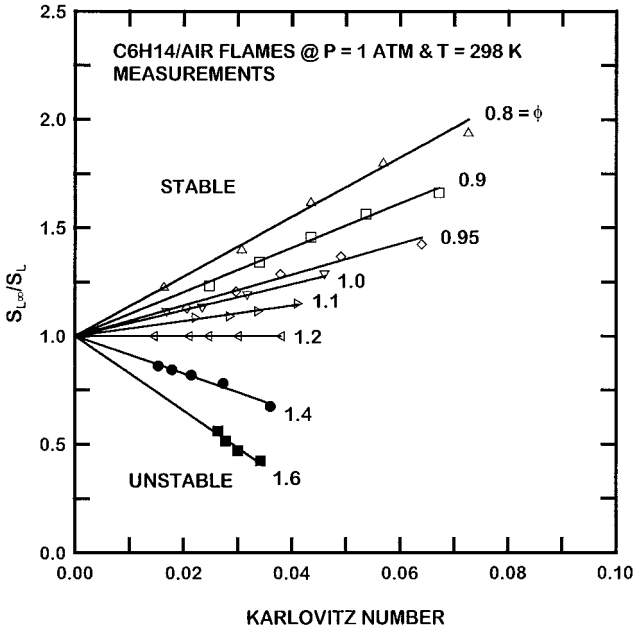

Fig. 1 Measured laminar burning velocities as a function of Karlovitz number and fuel-equivalence ratio for n-hexane/air flames at STP.

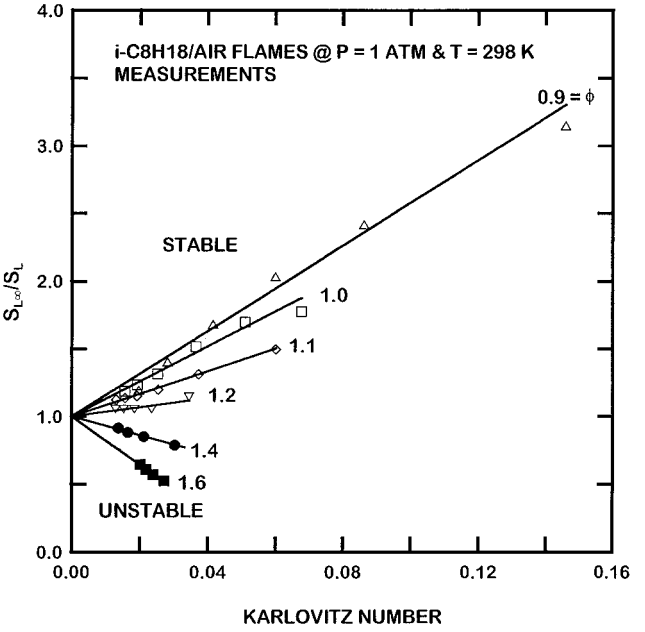

Fig. 3 Measured laminar burning velocities as a function of Karlovitz number and fuel-equivalence ratio for iso-octane/air flames at STP.

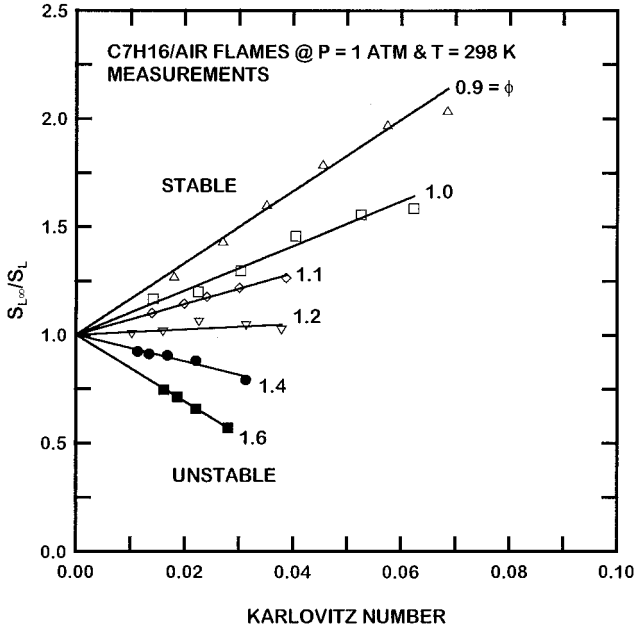

Fig. 2 Measured laminar burning velocities as a function of Karlovitz number and fuel-equivalence ratio for n-heptane/air flames at STP.

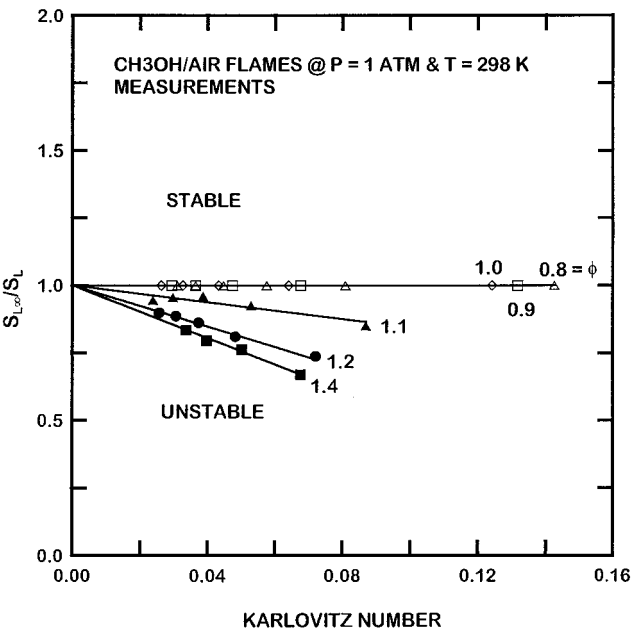

Fig. 4 Measured laminar burning velocities as a function of Karlovitz number and fuel-equivalence ratio for methyl-alcohol/air flames at STP.

burning velocities are indicated by open symbols whereas filled symbols indicate stretch-corrected results to find S_{L_∞}. Predictions are shown as lines, and all calculations were carried out for unstretched flames. Among the measurements, the results of Bradley et al.[10] were actually obtained at 358 K, whereas the results of Egolfopoulos et al.[27,28] have been extrapolated to 298 K from measurements at temperatures of 318–453 K; all other measurements shown in Figs. 6–10 are for an unburned gas temperature of 298 K.

Because of larger unburned gas temperatures, the stretch-corrected measurements of laminar burning velocities of Bradley et al.[10] for iso-octane (Fig. 8) are generally larger than the other stretch-corrected results for this fuel. The agreement between the remaining stretch-corrected laminar burning velocities of Davis and Law[29] and the present investigation for the various fuel vapors, however, is poorer than past observations of stretch-corrected laminar burning velocities for gaseous fuels. There are two major reasons for this behavior: Problems of vaporizing and mixing liquid fuels tend to increase experimental uncertainties, and extrapolation of the measurements of Egolfopoulos et al.[27,28] also increases experimental uncertainties. Comparisons between the stretch-corrected and uncorrected laminar burning velocities are hard to quantify because experimental uncertainties generally are not stated for the uncorrected measurements. The most consistent trend, however, is that the uncorrected laminar burning velocities tend to be larger than the stretch-corrected results. In view of the strong sensitivity of the present flames to stretch, however, differences between the stretch-corrected and uncorrected laminar burning velocities are surprisingly modest. In general, differences among the various predictions and measurements are comparable, suggesting less difficulties in predicting unstretched laminar burning velocities than other flame properties.

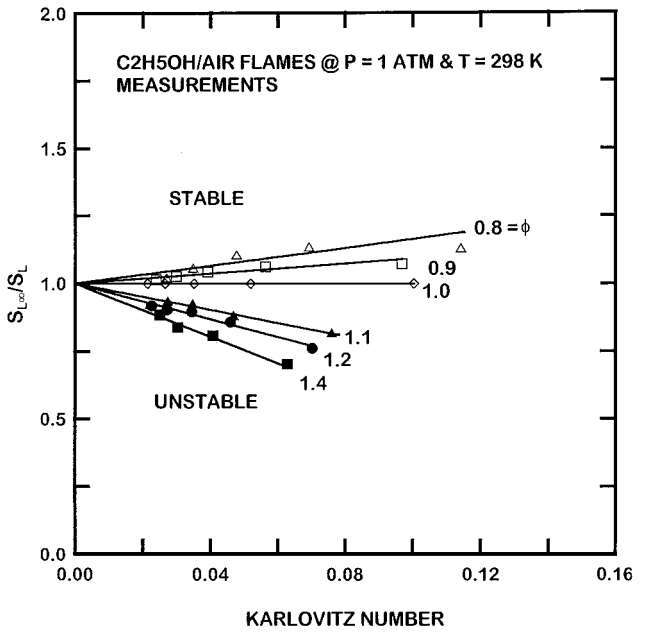

Fig. 5 Measured laminar burning velocities as a function of Karlovitz number and fuel-equivalence ratio for ethyl-alcohol/air flames at STP.

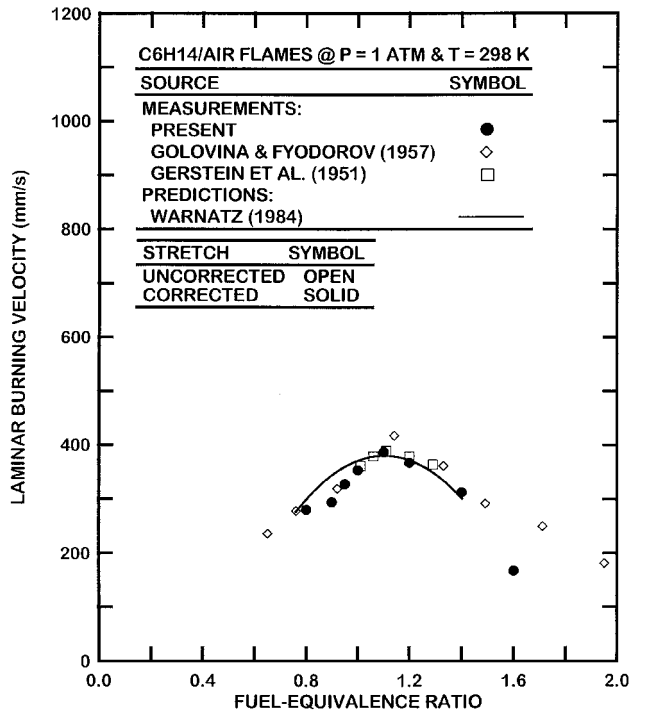

Fig. 6 Measured and predicted laminar burning velocities as a function of fuel-equivalence ratio for n-hexane/air flames at STP.

Markstein Numbers

Measurements and predictions of Markstein numbers for the fuel-vapor/air flames at atmospheric pressure are plotted in Fig. 11. Measurements shown in Fig. 11 include results from Bradley et al.[10] for iso-octane/air mixtures at an initial temperature of 358 K and the present measurements for all of the fuel vapors at an initial temperature of 298 K. Predictions of Müller et al.[35] for iso-octane/air mixtures at an initial temperature of 298 K are shown in Fig. 11; these predictions were obtained from a simplified analysis as opposed to the detailed mechanism summarized in Table 2. The agreement between the measurements of Bradley et al.[10] and the present investigation is very good in spite of the different initial temperatures; results considered later will show that the somewhat reduced values of Markstein numbers at the larger initial mixture temperature are quite reasonable. The predictions of Markstein numbers due to Müller et al.[35] are only qualitatively correct, which is typical of the performance of their simplified approach for other heavy hydrocarbons.[33,39]

The plots of Fig. 11 highlight the strong sensitivity of the paraffin-fueled flames to preferential diffusion/stretch interactions due to the rather large absolute values of these Markstein numbers, in the

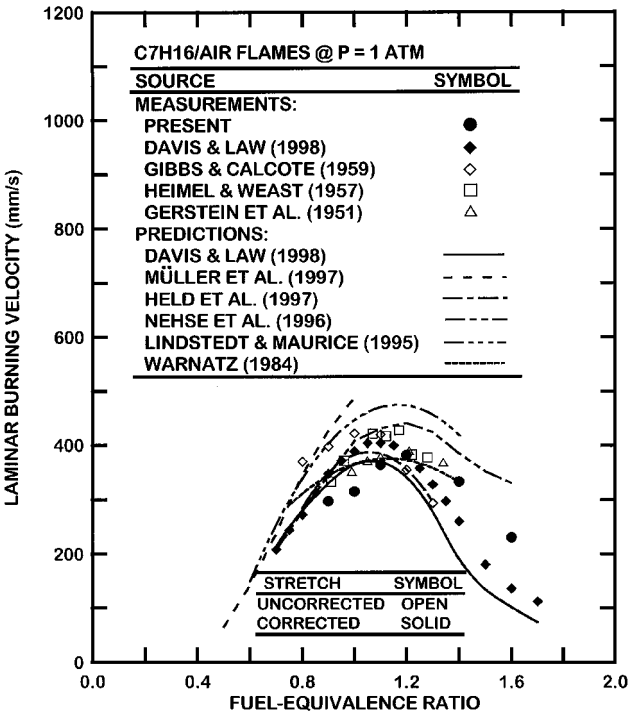

Fig. 7 Measured and predicted laminar burning velocities as a function of fuel-equivalence ratio for n-heptane/air flames at STP.

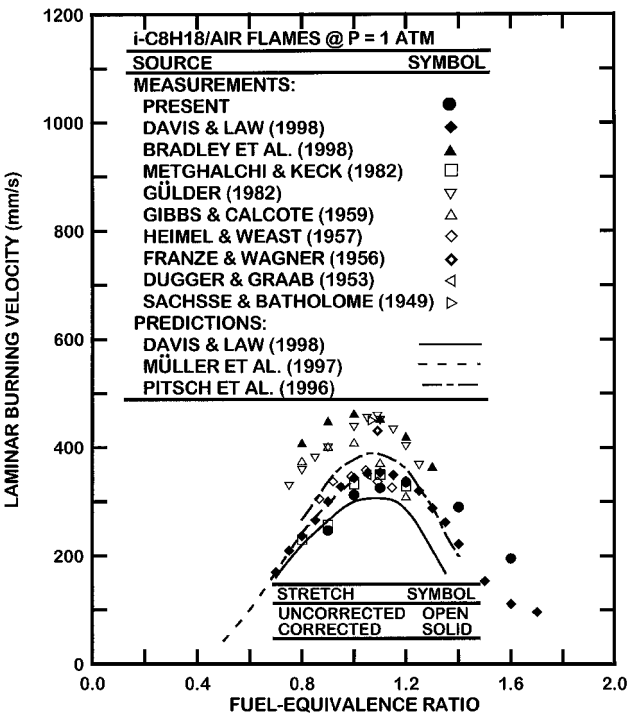

Fig. 8 Measured and predicted laminar burning velocities as a function of fuel-equivalence ratio for iso-octane/air flames at STP.

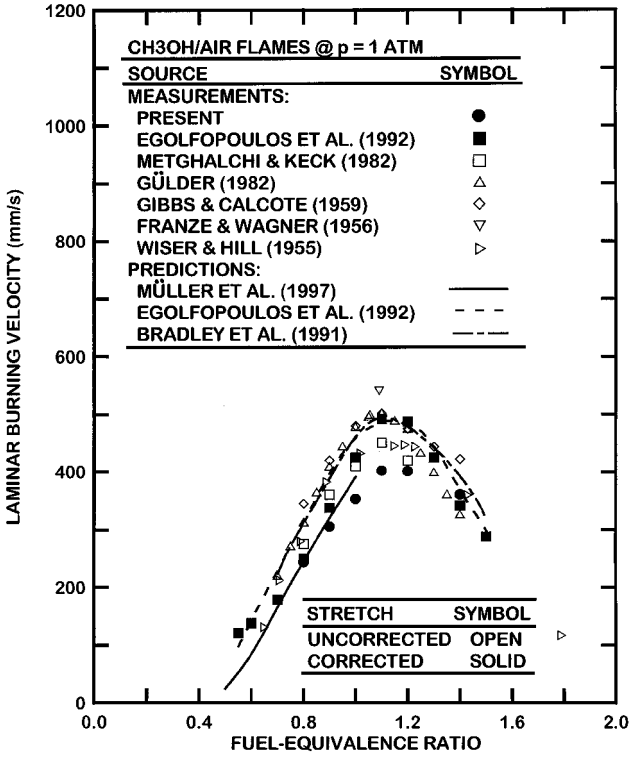

Fig. 9 Measured and predicted laminar burning velocities as a function of fuel-equivalence ratio for methyl-alcohol/air flames at STP.

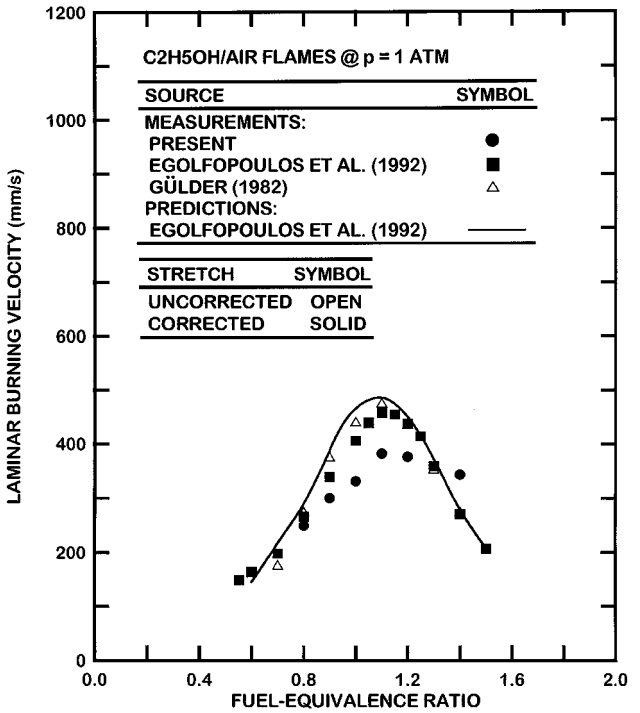

Fig. 10 Measured and predicted laminar burning velocities as a function of fuel-equivalence ratio for ethyl-alcohol/air flames at STP.

range from 30 to −20 after including the results of Bradley et al.[10] The corresponding sensitivity of the alcohol-fueled flames to preferential diffusion/stretch interactions is seen to be much weaker, with Markstein numbers only in the range from 0 to −5. The neutral preferential diffusion condition ($Ma = 0$) is observed for fuel-equivalence ratios of roughly 1.1–1.2 for all of the fuel vapors, which corresponds to the maximum laminar burning velocity conditions seen in Figs. 6–10. Finally, positive and negative Markstein

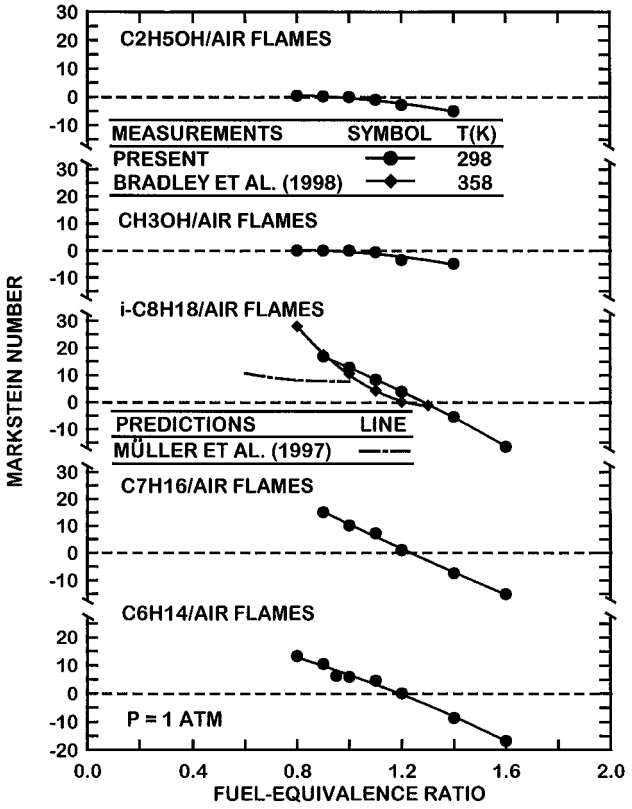

Fig. 11 Measured and predicted Markstein numbers as a function of fuel-equivalence ratio for liquid-fuel/air flames at STP.

numbers, associated with stable and unstable preferential diffusion behavior, are generally observed for fuel-lean and fuel-rich conditions, respectively. All of these trends are consistent with classical ideas about preferential diffusion/stretch interactions based on simple consideration of the preferential diffusion of the fuel compared to other major gas species.

n-Hexane/O_2/N_2 Flames at Standard Temperature

Potential Behavior of Practical Flames

Most practical premixed fuel-vapor/air flames operate with considerably larger flame temperatures and pressures than the test conditions considered thus far; therefore, it is not known whether the strong preferential diffusion/stretch interactions of the present flames with reactants at STP conditions persist to practical flame conditions. Effects of temperature on flame sensitivity to preferential diffusion/stretch interactions are not well known, but past studies for a variety of fuels suggest increased tendencies toward unstable flame behavior due to preferential diffusion effects with increasing pressure (see Hassan et al.[8,9] and references cited therein). Thus, to gain more insight about this issue, effects of flame temperature and pressure on the sensitivity of hydrocarbon flames to preferential diffusion/stretch interactions was studied experimentally considering n-hexane/O_2/N_2 reactant mixtures. This information was obtained by changes of flame temperatures by varying O_2 concentrations in the nonfuel gases at STP and by changing flame pressures for fuel/air mixtures at standard temperature. These results will be considered next.

Effect of Temperature on Flame Response to Stretch

Effects of flame temperature on flame response to stretch are shown in Figs. 12 and 13 for fuel-lean ($\phi = 0.8$) and stoichiometric conditions, respectively. Figures 12 and 13 consist of plots of unstretched laminar burning velocities and Markstein numbers as a function of oxygen concentration in the nonfuel gases. Increasing the flame temperature by increasing the oxygen concentration yields a corresponding increase of S_{L_∞}. This behavior follows because

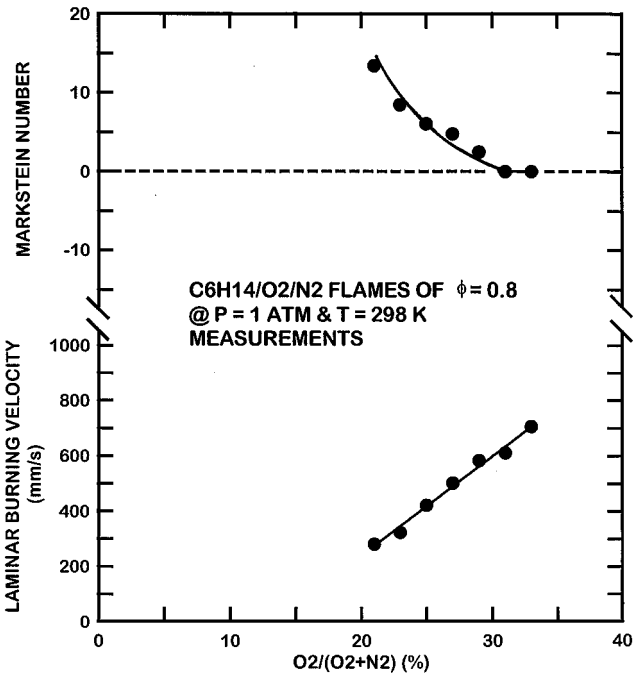

Fig. 12 Effect of oxygen concentration on measured laminar burning velocities and Markstein numbers of n-hexane/O_2/N_2 flames at a fuel-equivalence ratio of 0.8 and STP.

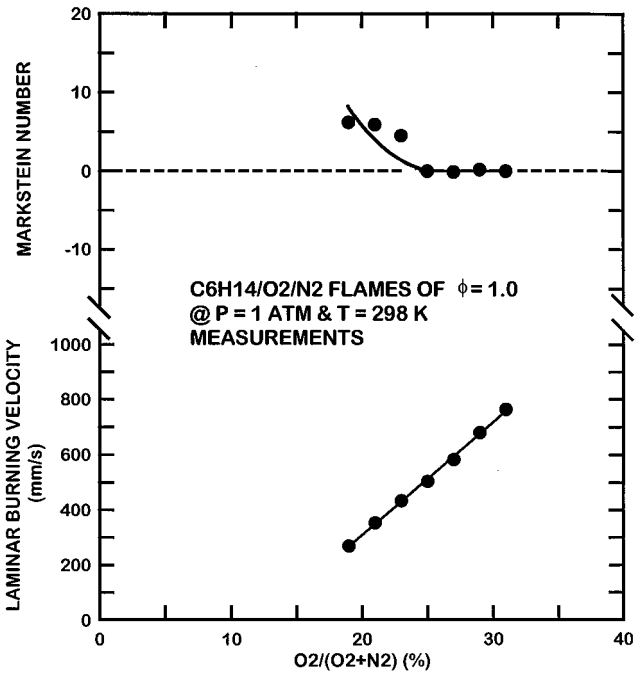

Fig. 13 Effect of oxygen concentration on measured laminar burning velocities and Markstein numbers of n-hexane/O_2/N_2 flames at a fuel-equivalence ratio of 1.0 and STP.

increased flame temperatures at a fixed pressure tend to increase radical concentrations in the reaction zone of the flame. Then, based on the well known proportionality between radical concentrations in the reaction zone and laminar burning velocities,[40] laminar burning velocities increase accordingly.

The corresponding variation of Markstein numbers with increasing flame temperatures seen in Figs. 12 and 13 is quite interesting. For both fuel-equivalenceratios, the Markstein numbers initially decrease with increasing flame temperature and then asymptotically approach $Ma = 0$. This behavior is particularly evident for stoichiometric conditions in Fig. 13, where initial values of the Markstein

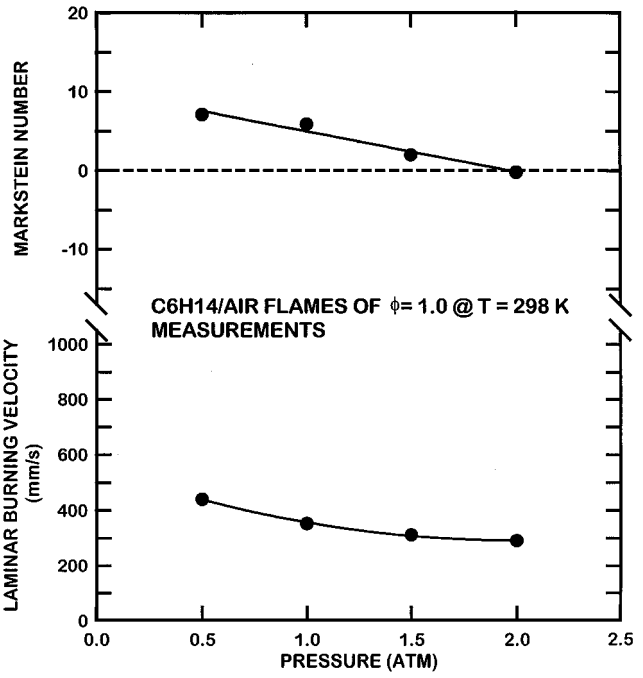

Fig. 14 Effect of pressure on measured laminar burning velocities and Markstein numbers of n-hexane/air flames at a fuel-equivalence ratio of 1.0 and a temperature of 298 K.

numbers are relatively small so that the range of oxygen concentrations where $Ma \approx 0$ is relatively broad. This behavior suggests that increased radical concentrations at increased flame temperatures tends to reduce the sensitivity of the present flames to effects of stretch.

Effect of Pressure on Flame Response to Stretch

Effects of flame pressure on flame response to stretch are shown in Fig. 14 for combustion in air at stoichiometric conditions. Figure 14 consists of plots of unstretched laminar burning velocities and Markstein numbers as a function of pressure. Increasing the flame pressure yields a progressive reduction of S_{L_∞}. This behavior follows due to increased rates of three-body recombination reactions with increasing pressure, which tends to reduce radical concentrations in the reaction zone of the flame. Then, the corresponding proportionality between radical concentrations in the reaction zone and laminar burning velocities,[40] discussed earlier, implies reduced laminar burning velocities with increasing pressure.

The associated variation of Markstein numbers with increasing pressure in Fig. 14 is generally similar to past observations for a variety of premixed flames (see Refs. 8 and 9 and references cited therein). In particular, Markstein numbers progressively decrease and become negative over wide ranges of fuel-equivalence ratios with increasing pressure, which enhances flame sensitivity to preferential-diffusion/stretch instability. This increased sensitivity for unstable behavior due to preferential diffusion/stretch interactions appears to be caused by reduced radical concentrations in the reaction zone, but the mechanism of this behavior is not known. In addition, whether the opposing effects of increased temperatures and increased pressures enhances or retards the sensitivity of practical flames to preferential diffusion/stretch interactions compared to laboratory experiments at STP remains an important open issue.

Conclusions

Effects of positive flame stretch on laminar burning velocities were studied experimentally for fuel-vapor/O_2/N_2 flames. The measurements were made for outwardly propagating spherical flames using methods developed earlier.[4–9] The major conclusions of the study are as follows.

1) Preferential diffusion/stretch interactions were conveniently correlated using the local conditions hypothesis, similar to past

work[4–9] because this yielded Markstein numbers that were relatively independent of Karlovitz numbers. Present observations were limited to Karlovitz numbers less than 0.2, however, and greater variations of Markstein numbers can be anticipated as quenching conditions are approached for Karlovitz numbers near unity.

2) Preferential diffusion/stretch interactions were substantial for heavy hydrocarbon vapors, yielding ratios of unstretched to stretched laminar burning velocities in the range 0.5–4.0, even for the present modest levels of stretch.

3) Various stretch-corrected measurements and predictions of unstretched laminar burning velocities exhibited poorer agreement for hydrocarbon-vapor flames than earlier results for gaseous hydrocarbon flames. This behavior is caused by increased experimental uncertainties due to problems of vaporizing and mixing liquid fuels and effects of extrapolating measurements at elevated temperatures to standard temperature conditions, as well as increased computational uncertainties due to less well developed chemical mechanisms for heavy hydrocarbon fuels.

4) Increasing flame temperatures tended to reduce flame sensitivity to stretch, whereas increasing pressures increased tendencies toward preferential diffusion instability behavior. Thus, whether the strong preferential diffusion/stretch interactions observed for heavy hydrocarbon flames at STP persist at the larger pressures and temperatures of most practical applications is an important unresolved issue.

5) Preferential diffusion instabilities were properly observed when Markstein numbers were negative and lead to the growth of irregular (chaotic) flame surface disturbances early in the flame propagation process; nevertheless, more regular (cellular) disturbances of flame surfaces, typical of hydrodynamic instabilities, were still observed at large flame radii when Markstein numbers were positive.

Acknowledgments

This research was supported in part by National Science Foundation Grants CTS-9019813 and 9321959 under the technical management of M. J. Linevsky and F. Fisher. Support from the Rackham Fellowship Program of the University of Michigan for O. C. Kwon and the Peace Fellowship Program of Egypt for M. I. Hassan is also gratefully acknowledged.

References

[1]Dowdy, D. R., Smith, D. B., Taylor, S. C., and Williams, A., "The Use of Expanding Spherical Flames to Determine Burning Velocities and Stretch Effects on Hydrogen/Air Mixtures," *Proceedings of the Twenty-Third International Symposium on Combustion*, Combustion Inst., Pittsburgh, PA, 1990, pp. 325–333.

[2]Brown, M. J., McLean, I. C., Smith, D. B., and Taylor, S. C., "Markstein Lengths of CO/H_2/Air Flames, Using Expanding Spherical Flames," *Proceedings of the Twenty-Sixth International Symposium on Combustion*, Combustion Inst., Pittsburgh, PA, 1996, pp. 875–882.

[3]Karpov, V. P., Lipatnikov, A. N., and Wolanski, P., "Finding the Markstein Number Using the Measurements of Expanding Spherical Laminar Flames," *Combustion and Flame*, Vol. 109, No. 3, 1996, pp. 436–448.

[4]Kwon, S., Tseng, L.-K., and Faeth, G. M., "Laminar Burning Velocities and Transition to Unstable Flames in $H_2/O_2/N_2$ and $C_3H_8/O_2/N_2$ Mixtures," *Combustion and Flame*, Vol. 90, No. 3, 1992, pp. 230–246.

[5]Tseng, L.-K., Ismail, M. A., and Faeth, G. M., "Laminar Burning Velocities and Markstein Numbers of Hydrocarbon/Air Flames," *Combustion and Flame*, Vol. 95, No. 4, 1993, pp. 410–426.

[6]Aung, K. T., Tseng, L.-K., Ismail, M. A., and Faeth, G. M., "Response to Comment by S. C. Taylor and D. B. Smith on 'Laminar Burning Velocities and Markstein Numbers of Hydrocarbon/Air Flames,'" *Combustion and Flame*, Vol. 102, No. 4, 1995, pp. 526–530.

[7]Aung, K. T., Hassan, M. I., and Faeth, G. M., "Flame/Stretch Interactions of Laminar Premixed Hydrogen/Air Flames at Normal Temperature and Pressure," *Combustion and Flame*, Vol. 109, No. 1/2, 1997, pp. 1–24.

[8]Hassan, M. I., Aung, K. T., and Faeth, G. M., "Measured and Predicted Properties of Laminar Premixed Methane/Air Flames at Various Pressures," *Combustion and Flame*, Vol. 115, No. 4, 1998, pp. 539–550.

[9]Hassan, M. I., Aung, K. T., Kwon, O. C., and Faeth, G. M., "Properties of Laminar Premixed Hydrocarbon/Air Flames at Various Pressures," *Journal of Propulsion and Power*, Vol. 14, No. 4, 1998, pp. 479–488.

[10]Bradley, D., Hicks, R. A., Lawes, M., Sheppard, C. G. W., and Woolley, R., "The Measurement of Laminar Burning Velocities and Markstein Numbers for Iso-Octane-Air and Iso-Octane-n-Heptane in Air Mixtures at Elevated Temperatures and Pressures in an Explosion Bomb," *Combustion and Flame*, Vol. 115, No. 1/2, 1998, pp. 126–144,

[11]Markstein, G. H., *Non-Steady Flame Propagation*, Pergamon, New York, 1964, p. 22.

[12]Strehlow, R. A., and Savage, L. D., "The Concept of Flame Stretch," *Combustion and Flame*, Vol. 31, No. 2, 1978, pp. 209–211.

[13]McBride, B. J., Reno, M. A., and Gordon, S., "CET93 and CETPC: An Interim Updated Version of the NASA Lewis Computer Program for Calculating Complex Chemical Equilibrium with Applications," NASA TM 4557, 1994.

[14]Reynolds, W. C., "The Element Potential Method for Chemical Equilibrium Analysis: Implementation in the Interactive Program STANJAN," Dept. of Mechanical Engineering Rept., Stanford Univ., Stanford, CA, 1986.

[15]Von Sachsse, H., and Bartholome, E., "Beiträge zen Frage der Flammengeschwindigkeit," *Zeitschrift für Elektrochemie*, Vol. 53, No. 4, 1949, pp. 183–190.

[16]Gerstein, M., Levine, O., and Wong, E. L., "The Determination of Fundamental Burning Properties of Hydrocarbons by a Revised Tube Method," *Journal of the American Chemical Society*, Vol. 73, No. 1, 1951, pp. 418–422.

[17]Dugger, G. L., and Graab, D. D., "Flame Velocities of Hydrocarbon-Oxygen-Nitrogen Mixtures," *Proceedings of the Fourth International Symposium on Combustion*, Combustion Inst., Pittsburgh, PA, 1952, pp. 302–310.

[18]Wiser, W. H., and Hill, G. R., "A Kinetic Comparison of the Combustion of Methyl Alcohol and Methane," *Proceedings of the Fifth International Symposium on Combustion*, Combustion Inst., Pittsburgh, PA, 1954, pp. 553–558.

[19]Van Franze, C., and Wagner, H. G., "Ausbreitung Laminarer Flammen in Vorgemischten Gasen: Messungen und Theorie der Flammengeschwindigheit," *Zeitschrift für Electrochemie*, Vol. 60, No. 6, 1956, pp. 525–556.

[20]Heimel, S., and Weast, R. C., "Effect of Initial Mixture Temperature on the Burning Velocity of Benzene-Air, n-Heptane-Air, and Iso-Octane-Air Mixtures," *Proceedings of the Sixth International Symposium on Combustion*, Combustion Inst., Pittsburgh, PA, 1956, pp. 296–302.

[21]Golovina, E. S., and Fyodorov, G. G., "Influence of Physical and Chemical Factors on Burning Velocity," *Proceedings of the Sixth International Symposium on Combustion*, Combustion Inst., Pittsburgh, PA, 1956, pp. 88–96.

[22]Gibbs, G. J., and Calcote, H. F., "Effect of Molecular Structure on Burning Velocity," *Journal of Chemical Engineering Data*, Vol. 4, 1959, pp. 226–237.

[23]Gülder, O. L., "Laminar Burning Velocities of Methanol, Ethanol and Iso-Octane-Air Mixtures," *Proceedings of the Nineteenth International Symposium on Combustion*, Combustion Inst., Pittsburgh, PA, 1982, pp. 275–281.

[24]Metghalchi, M., and Keck, J. C., "Burning Velocity of Mixtures of Air with Methanol, Isooctane, and Indolene at High Pressure and Temperature," *Combustion and Flame*, Vol. 48, No. 2, 1982, pp. 191–210.

[25]James, E. H., "Laminar Burning Velocities of Iso-Octane-Air Mixtures—A Literature Review," Society of Automotive Engineers, Paper 870170, 1987.

[26]Bradley, D., Dixon-Lewis, G., Habik, S. E., Kwa, L. K., and El-Sherif, S., "Laminar Flame Stucture and Burning Velocities of Premixed Methanol-Air," *Combustion and Flame*, Vol. 85, Nos. 1–2, 1991, pp. 105–120.

[27]Egolfopoulos, F. N., Du, D. X., and Law, C. K., "A Comprehensive Study of Methanol Kinetics in Freely-Propagating and Burner-Stabilized Flames, Flow and Static Reactors, and Shock Tubes," *Combustion Science Technology*, Vol. 83, Nos. 1–3, 1992, pp. 33–75.

[28]Egolfopoulos, F. N., Du, D. X., and Law, C. K., "A Study of Ethanol Oxidation Kinetics in Laminar Premixed Flames, Flow Reactors, and Shock Tubes," *Proceedings of the Twenty-Fourth International Symposium on Combustion*, Combustion Inst., Pittsburgh, PA, 1992, pp. 833–841.

[29]Davis, S. G., and Law, C. K., "Laminar Flame Speeds and Oxidation Kinetics of Iso-Octane/Air and n-Heptane/Air Flames," *Proceedings of the Twenty-Seventh International Symposium on Combustion*, Combustion Inst., Pittsburgh, PA, 1998, pp. 521–527.

[30]Warnatz, J., "Chemistry of High Temperature Combustion of Alkanes up to Octane," *Proceedings of the Twentieth International Symposium on Combustion*, Combustion Inst., Pittsburgh, PA, 1984, pp. 845–856.

[31]Lindstedt, R. P., and Maurice, L. Q., "Detailed Kinetic Modeling of n-Heptane Combustion," *Combustion Science Technology*, Vol. 107, Nos. 4–6, 1995, pp. 317–353.

[32]Nehse, M., Warnatz, J., and Chevalier, G., "Kinetic Modeling of the Oxidation of Large Aliphatic Hydrocarbons," *Proceedings of the Twenty-Sixth International Symposium on Combustion*, Combustion Inst., Pittsburgh, PA, 1996, pp. 773–780.

[33]Pitsch, H., Peters, N., and Seshadri, K., "Numerical and Asymptotic Studies of the Structure of Premixed Iso-Octane Flames," *Proceedings of the Twenty-Sixth International Symposium on Combustion*, Combustion Inst., Pittsburgh, PA, 1996, pp. 763–771.

[34]Held, T. J., Marchese, A. J., and Dryer, F. L., "A Semi-Empirical Reaction Mechanism for n-Heptane Oxidation and Pyrolysis," *Combustion Science Technology*, Vol. 123, Nos. 1–5, 1997, pp. 107–146.

[35]Müller, U. C., Bolling, M., and Peters, N., "Appoximations for Burning Velocities and Markstein Numbers for Lean Hydrocarbon and Methanol Flames," *Combustion and Flame*, Vol. 108, No. 3, 1997, pp. 349–356.

[36]Groff, E. G., "The Cellular Nature of Confined Spherical Propane–Air Flames," *Combustion and Flame*, Vol. 48, No. 1, 1982, pp. 51–62.

[37]Manton, J., von Elbe, G., and Lewis, B., "Nonisotropic Propagation of Combustion Waves in Explosive Gas Mixtures and Development of Cellular Flames," *Journal of Chemical Physics*, Vol. 20, 1952 , pp. 153–158.

[38]Law, C. K., "Dynamics of Stretched Flames," *Proceedings of the Twenty-Second International Symposium on Combustion*, Combustion Inst., Pittsburgh, PA, 1988, pp. 1381–1402.

[39]Kwon, O.-C., Aung, K. T., Tseng, L.-K., Ismail, M. A., and Faeth, G. M., "Comment on 'Approximations for Burning Velocities and Markstein Numbers for Lean Hydrocarbon and Methanol Flames' by U. C. Müller, B. Bollig, and N. Peters," *Combustion and Flame*, Vol. 116, No. 1-2, 1999, pp. 310–312.

[40]Padley, P. J., and Sugden, T. M., "Chemiluminescence and Radical Recombination in Hydrogen Flames," *Proceedings of the Seventh International Symposium on Combustion*, Combustion Inst., Pittsburgh, PA, 1958, pp. 235–244.